JOURNAL OF Applied Polymer SCIENCE

Synergistic toughening effect of chlorinated polyethylene and acrylic resin on SAN/ASA blends at low temperature

Zepeng Mao,[1,2] Jun Zhang[1,2]

[1]Department of Polymer Science and Engineering, College of Materials Science and Engineering, Nanjing Tech University, Nanjing 210009, China

[2]Jiangsu Collaborative Innovation Center for Advanced Inorganic Function Composites, Nanjing 210009, China

Correspondence to: J. Zhang (E-mail: zhangjun@njtech.edu.cn)

ABSTRACT: Styrene–acrylonitrile copolymer (SAN)/acrylonitrile–styrene–acrylate terpolymer (ASA) blends (75/25, w/w) were toughened by blending with chlorinated polyethylene (CPE) and acrylic resin (ACR) at three different temperatures (−30, 0, and 25 °C). When the testing temperature was 0 and 25 °C, CPE played a key role in improving the impact strength of blends instead of ACR. However, an obvious synergistic toughening effect of CPE and ACR was observed at −30 °C: when both 10 phr CPE and 15 phr ACR were added, the impact strength of the blends reached a peak at 7.50 kJ/m^2, which was about two to three times higher than when 25 phr CPE or 25 phr ACR was introduced into the blends individually. Scanning electron microscopy, dynamic mechanical analysis, and surface energy measurements were used to investigate the toughening mechanism. Furthermore, other mechanical properties and the heat distortion temperatures were evaluated. © 2016 Wiley Periodicals, Inc. J. Appl. Polym. Sci. **2016**, *133*, 43958.

KEYWORDS: blends; copolymers; glass transition; properties and characterization

Received 28 February 2016; accepted 12 May 2016

DOI: 10.1002/app.43958

INTRODUCTION

The impact toughness of polymer materials is not only an important factor in characterizing the mechanical properties but also a main factor considered for applications. In fact, when a polymer material is used outdoors in winter, the service temperature can be even lower than −30 °C. Therefore, when we toughen a material, both room temperature and lower temperatures should be taken into account. Thus it would be of interest to study the toughness of plastics at different temperatures.

Styrene–acrylonitrile copolymer (SAN), an engineering thermoplastic material, has many outstanding properties,[1] such as good mechanical properties, weather resistance, chemical resistance, and easy processing characteristics. It has many important applications, such as the fittings of mobile industry and home appliances, instrument panels, and various switches and lamina of the fanner. Acrylonitrile–styrene–acrylate terpolymer (ASA) is a core–shell-structured polymer,[2,3] which is obtained by grafting a SAN shell onto a crosslinked poly(*n*-butyl acrylate) (PnBA) rubber core. ASA has been considered as an ideal substitute for acrylonitrile–butadiene–styrene copolymer (ABS) since the acrylate component in ASA is more resistant to the attack of ultraviolet radiation and oxygen in comparison with the unsaturated butadiene component in ABS.[4,5]

In industry, SAN is often blended with ASA to prepare ASA resin, which possesses excellent rigidity, heat resistance, and advanced weather resistance. However, the incorporation of ASA fails to offer a satisfactory increase in the toughness of brittle SAN.[6] In our previous work,[7] chlorinated polyethylene (CPE) was used to toughen the SAN/ASA (75/25) binary blends. The addition of CPE was effective in improving the impact toughness of the SAN/ASA (75/25) binary blends at 23 and 0 °C. The impact strength increased by 11 times at 23 °C and 10 times at 0 °C with the addition of 60 phr CPE. Nevertheless, the toughening effect was not obvious when the testing temperature was −30 °C. The main reason is that the polymeric chains of CPE have been "frozen out" at −30 °C, so the CPE evidently cannot improve the toughness of the blends.

Acrylic resin (ACR) is a typical core–shell-structured impact modifier and is largely used in toughening rigid plastics, especially in improving the low-temperature toughness of poly(vinyl chloride) (PVC) even as low as −40 °C.[8–10] The poly(butyl acrylate) (PBA) rubbery core in ACR particles is the dominant toughening material, and the thin shell phase that consists of poly(methyl methacrylate) (PMMA) can effectively enhance the interfacial adhesion between the core and matrix. In our previous work,[11] ACR was used to toughen the SAN/ASA binary blends at room temperature. The results showed that SAN/ASA/

ACR blends have good compatibility, and a ductile–brittle transition was observed in the blends.

Here, considering that the impact toughness of blends at 25 and 0 °C could be improved by CPE and that at −30 °C could be improved by ACR, we first added ACR and CPE to SAN/ASA (75/25) blends, followed by detecting whether a synergistic toughening effect exists between CPE and ACR. The goal is to prepare a blend that has good impact toughness at all three temperatures (−30, 0, and 25 °C) by combining different impact modifiers.

EXPERIMENTAL

Materials

SAN (D-178) was supplied by Zhenjiang GPPC Chemical Co., Ltd. (Zhenjiang, China). ASA (HX-960) was supplied by Zibo Huaxing Additives Co., Ltd. (Zibo, China). CPE (135A, with 36 wt % Cl content) was produced by Weifang Yaxing Chemical Co., Ltd. (Weifang, China). ACR (FM-50) was obtained from Kanegafuchi Chemical Industry Co., Ltd., (Tokyo, Japan). Other additives, such as Irganox B215, calcium stearate, and polyethylene wax, were all industrial grade and used as antioxidant, external lubricant, and internal lubricant, respectively.

Sample Preparation

In order to estimate the possible interaction between CPE and ACR, SAN/ASA was fixed at a weight ratio of 75/25 to be the matrix, with the ratio of CPE/ACR content varying from 0/25 to 25/0. Thus the blends of SAN/ASA/CPE/ACR were described as 75/25/x/y (x and $y = 0$, 5, 10, 15, 20, 25). The samples were designated as CxAy, where C and A represented CPE and ACR, and x and y represented their dosages, respectively.

The blends and all the additives were mixed by a two-roll mill (SK-160B, Shanghai Rubber Machinery Works, Shanghai, China) at 180 °C. SAN, ASA, and the additives were first melted for 2 min, and then the mixture of CPE and ACR was added and continued to mix for 8 min.[7] After that, the compounds were compression-molded into 2 and 4 mm thick sheets in a plate vulcanizing press (XLB-D 350 × 350 × 2, Shanghai First Rubber Machinery Factory, Shanghai, China) at 180 °C for 15 min under a pressure of 10 MPa. The mold was allowed to cool under the same pressure to room temperature before removing the sheets from the mold. The dumbbell-shaped specimens cut from 2 mm sheets were used for tensile testing, and rectangular specimens (80 × 10 × 4 mm^3) cut from sheets 4 mm thick were used for flexural, impact, and heat distortion temperature tests. All the specimens including dumbbell and rectangular shapes were annealed at 120 °C for 2 h.

Impact Property

The notched Izod impact strength was carried out following ISO 180 (Plastics: Determination of Izod Impact Strength)[12] on an Izod impact tester (UJ-4, Chengde Machine Factory, Chengde, China). According to the standard, the testing specimens (80 × 10 × 4 mm^3) were made as notch type A, which has a notch base radius of 0.25 ± 0.05 mm, a notch angle of 45 ± 1°, and a remaining width at the notch base of 8.0 ± 0.2 mm. The above test was conducted at three different temperatures (25, 0, and −30 °C). Before testing, the specimens were kept at the corresponding temperature for 10 h in order to rule out any temperature errors. The test at 25 °C was conducted in an air-conditioned room. As to the tests at 0 and −30 °C, the samples were first chilled for 10 h in a refrigerator where the temperature had already been set, and then the samples were taken out of the refrigerator to test instantly.

Scanning Electron Microscopy Analysis

Scanning electron microscopy (SEM; JSM-5900; JEOL, Tokyo, Japan) was used to observe the impact-fractured surfaces of the blends with an accelerating voltage of 15 kV. The fracture surfaces of the samples were coated with a thin conductive layer of gold before scanning. No staining or any other chemical treatments were used in this test.

Dynamic Mechanical Analysis

The dynamic thermal analysis was performed by a modular compact rheometer (MCR302, Anton Paar, Graz, Austria). The dynamic mechanical analysis (DMA) of the blends was scanned in the torsion mode at a constant frequency of 1 Hz, an amplitude of 0.05%, and a temperature range from −90 to 160 °C at a heating rate of 3 °C/min. All the samples (30 × 6 × 2 mm^3) were cut from compression-molded sheets. The storage modulus (G') and loss tangent (tan δ) were obtained as a function of temperature for all the samples under identical test conditions. The glass-transition temperature (T_g) was defined as the peak of the tan δ curves.

Contact Angle Measurements

The contact angles were measured in a DSA 100 drop shape analysis system (Krüss, Hamburg, Germany) at room temperature. The tested specimens were obtained via compression molding. Two test liquids [distilled water (H_2O) and diiodomethane (CH_2I_2)] were selected, and the contact angle was recorded 30 s after 2.0 μL of solvent was dropped onto the surface of the sample. The contact angle values of the samples in this study were the average of at least five repetitive tests on the same sample. The standard deviations of the contact angle values were calculated as less than ±2°.

Flexural and Tensile Properties

Flexural and tensile tests were carried out on a universal testing machine (CMT 5254, Shenzhen SANS Testing Machine Co., Ltd., Shenzhen, China) according to ISO 178 (Plastics: Determination of Flexural Properties)[13] and ISO 527 (Plastics: Determination of Tensile Properties)[14] with an invariant rate of 2 and 5 mm/min, respectively. Both tests were performed at room temperature (25 °C).

Heat Distortion Temperature

The heat distortion temperatures (HDT) of the blends were evaluated with Vicat/HDT equipment (ZWK 1302-2, Shenzhen SANS Testing Machine Co., Ltd., Shenzhen, China). All tests were conducted at a heating rate of 120 °C/h under the maximum blending stress of 1.80 and 0.45 MPa, following ISO 75 (Plastics: Determination of Temperature of Deflection under Load).[15]

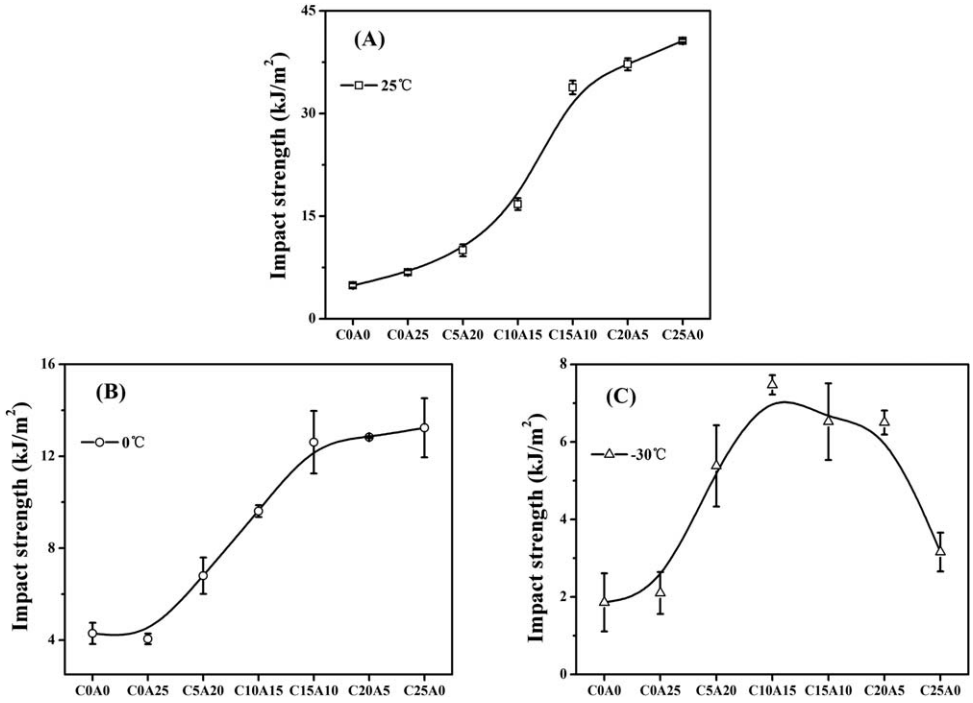

Figure 1. Notched Izod impact strengths of SAN/ASA/CPE/ACR blends at different temperatures.

RESULTS AND DISCUSSION

Impact Property

In order to explore whether CPE and ACR have a synergistic toughening effect in SAN/ASA (75/25) blends, the ratio of CPE/ACR content was varied from 0/25 to 25/0. The impact strengths of the blends at three temperatures (−30, 0, and 25 °C) are exhibited in Figure 1. As shown in Figure 1(A), when the 25 phr ACR is added to SAN/ASA (75/25) blends alone, the impact strength is low (6.79 kJ/m^2) at 25 °C. With the increase of CPE concentration, the impact strength grows constantly, and a ductile–brittle transition is observed when CPE and ACR are close to the same content. The maximum value of 40.63 kJ/m^2 appears at C25A0, which is nearly six times higher than the impact strength of C0A25. A similar increasing trend is

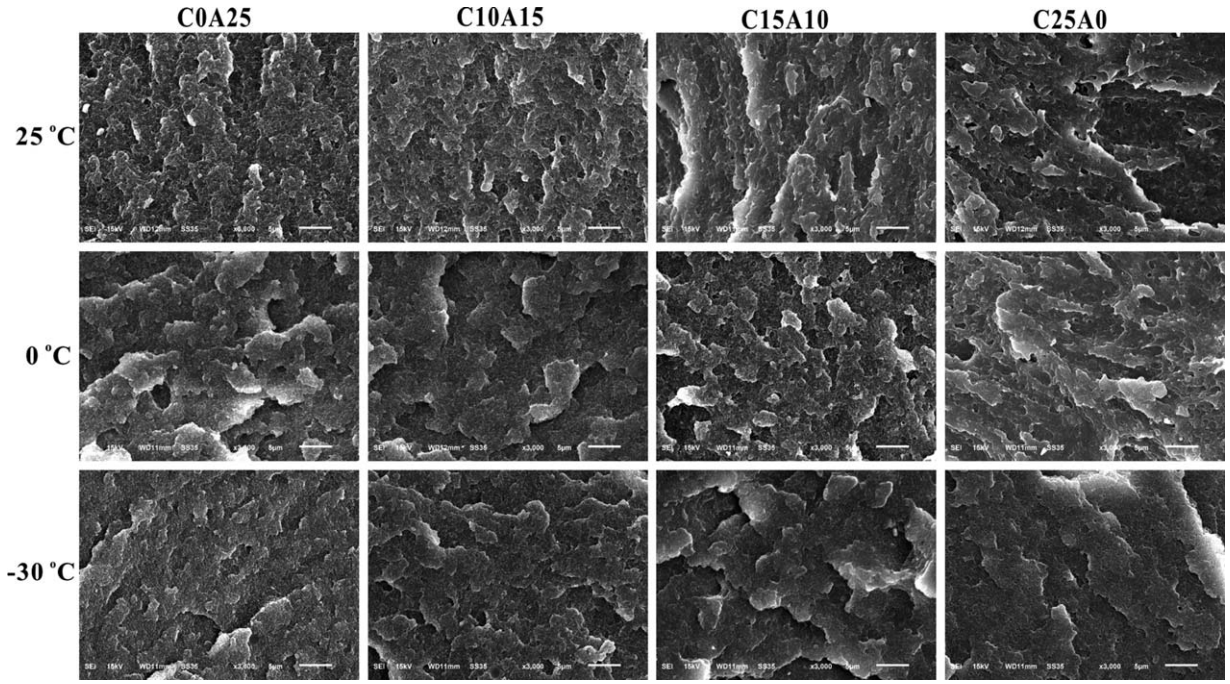

Figure 2. SEM photographs of fracture surfaces of SAN/ASA/CPE/ACR blends.

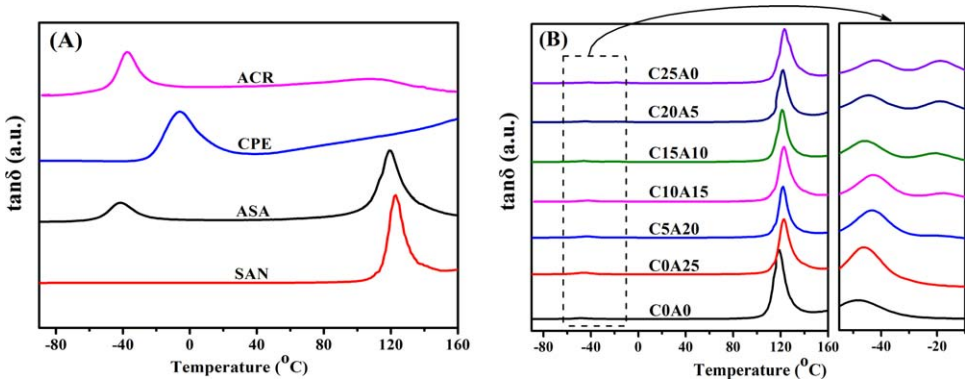

Figure 3. The tan δ curves of SAN, ASA, CPE, ACR, and SAN/ASA/CPE/ACR blends. [Color figure can be viewed in the online issue, which is available at wileyonlinelibrary.com.]

observed at 0 °C in Figure 1(B). When the CPE content increases to 15 phr, the impact strength is maintained at around 13 kJ/m^2 and almost does not change. However, introducing ACR individually to SAN/ASA (75/25) blends evidently cannot improve the impact strength at 0 and 25 °C. That is to say, the CPE plays a major role in improving the impact strength of the blends at 0 and 25 °C.

Surprisingly, an obvious synergistic toughening effect of CPE and ACR appeared at −30 °C. The impact strength of the blends is low when the CPE or ACR is added alone, whereas it increases noticeably when the CPE couples with ACR. For example, when the CPE and ACR are close to the same content, the impact strength of the blends reaches a peak of about 7.50 kJ/m^2, which is about two to three times higher than for C25A0 or C0A25.

Furthermore, it should be noted that when 15 phr CPE and 10 phr ACR are both added, the blends have a good toughness at all three temperatures (−30, 0, and 25 °C), where the impact strengths are 6.52, 12.61, and 33.81 kJ/m^2, respectively.

SEM Analysis

SEM micrographs with the same magnification show the fracture surfaces of samples after impact tests. In our previous work, ACR was used to toughen the SAN/ASA binary blends individually.[11] The results showed that SAN/ASA/ACR blends have good compatibility. Since a ductile–brittle transition was observed in the SAN/ASA/ACR blends, the addition of ACR could only enhance the toughness on a limited scale, such that the impact strength of SAN/ASA/ACR (70/30/30) blends was only 6.9 kJ/m^2. As shown in Figure 2, a surface mainly composed of tiny separating platelets and a cloud-shaped structure is observed in C0A25 at 25 °C, which is a typical fracture surface for the core–shell impact modifier toughened plastics.[16,17] With the increase of CPE dosage, the fracture surface is rather coarse, and a thread-like morphology appears once the CPE content is over 15 phr. When 25 phr CPE is added alone at 25 °C, the impact-fractured surface shows an obvious thread-like morphology, and some microholes are clearly found on the surface, indicating a favorable toughening effect.

According to the literature,[8] when ACR was applied for plastics toughening, it acted as a stress concentrator in blends and induced a large number of crazes during the deformation process, leading to the appearance of a cloud-shaped surface. Whereas, after the CPE was introduced into plastics,[16] an approximate network structure formed in the polymer matrix, tending to form shear bands to absorb energy, and a fiber-like or thread-like morphology always appeared. These conclusions are verified by the SEM photographs in this study. Moreover, according to the Figure 2, cloud-shaped and thread-like structures emerge synchronously when both CPE and ACR are introduced at 25 °C, such as in C10A15 and C15A10. With respect to 0 °C, a tendency similar to that at 25 °C appears.

It should be pointed out that the morphology like at 25 or 0 °C disappears at −30 °C. The toughness of the impact-fractured surface increases in the first stage and then decreases. Correlating well with the impact results, the micrographs of C10A15 and C15A10 are rougher than both the left and right sides at −30 °C. Overlapped platelets arise at the impact-fractured

Table I. Glass-Transition Temperatures of Blends from tan δ Curves

Sample	$T_{g,1}$ (°C)	$T_{g,2}$ (°C)	$T_{g,3}$ (°C)	Sample	$T_{g,1}$ (°C)	$T_{g,2}$ (°C)	$T_{g,3}$ (°C)
SAN	—	—	122.8	C0A0	−48.3	—	118.7
ASA	−41.9	—	119.0	C0A25	−45.9	—	122.9
ACR	−37.6	—	107.0	C5A20	−43.2	−20.6	121.7
CPE	—	−6.3	—	C10A15	−42.7	−18.2	123.0
				C15A10	−45.9	−21.0	121.0
				C20A5	−44.4	−18.5	122.0
				C25A0	−42.0	−18.8	123.0

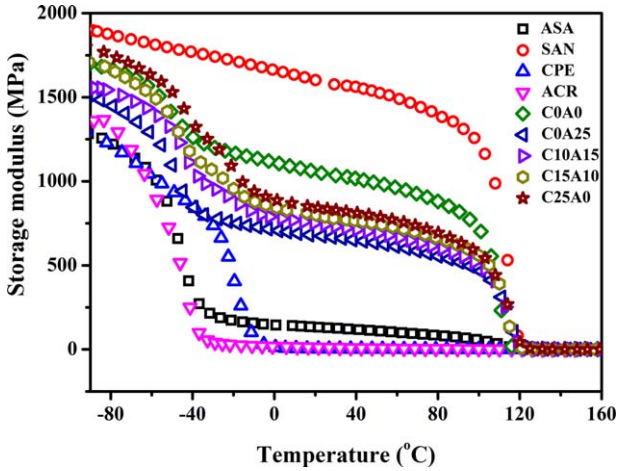

Figure 4. Storage modulus curves of SAN/ASA/CPE/ACR blends. [Color figure can be viewed in the online issue, which is available at wileyonlinelibrary.com.]

surface of C10A15 and C15A10 at −30 °C, while the impact-fractured surfaces of C0A25 and C25A0 are relatively smooth, indicating that ACR plays a major role in improving the impact strength instead of the CPE. In other words, all the results obtained from SEM analysis are in great agreement with the impact strength of the blends.

Dynamic Mechanical Analysis

The glass-transition behaviors of the blends were recorded by DMA. The tan δ curves of pure SAN, ASA, CPE, ACR, and the SAN/ASA/CPE/ACR blends with different compositions are shown in Figure 3. The peak temperatures of the tan δ curves are defined as the T_g values of the corresponding components, and the derived results are summarized in Table I.

It can be observed that both SAN and CPE show only one glass-transition temperature, while two glass transitions are detected in ASA and ACR. It is well known that traditional core–shell-structured polymers show two glass-transition temperatures from DMA analysis: the lower temperature peak belongs to the rubber phase, and the higher temperature peak belongs to the rigid shell. Therefore, from the tan δ curves of ASA, the T_g in the low-temperature region (−41.9 °C) is consistent with the PnBA core, and the T_g in the high-temperature region (119.0 °C) is attributed to the SAN shell. With regard to ACR, similarly, the two glass transitions (−37.6 and 107.0 °C) correspond to the PBA rubber core and the PMMA rigid shell, respectively. Comparing all of the $T_{g,2}$ values of Table I, there is a significant value dropping from pure CPE (−6.3 °C) to CPE components (−21.0 to −18.2 °C) in blends. The same phenomenon has been reported previously.[7,18,19] The negative pressure created by the difference in thermal expansion coefficients of the soft and hard phases might be responsible for this decrease.[20]

After blending of SAN and ASA, the T_g in the low-temperature region of the binary blends (C0A0) decreases from −41.9 to −48.3 °C. The possible reason is that the addition of SAN diluted the acrylate concentration and expanded the motion space of the rubber phase.[21] Therefore, the chain segments began to move at a relatively lower temperature, and a decrease of the T_g was observed.

Moreover, when CPE and ACR are introduced into SAN/ASA blends, the T_g values in the low-temperature region are maintained at about −18 and −45 °C, respectively, and no obvious excursion is observed. Because of the good compatibility between SAN and PMMA[22] and the close values of their T_g, the blends show only one T_g at about 120 °C in the high-temperature region.

As shown in Figure 4, the storage modulus of rigid polymer SAN is the highest, while the three elastomers are pretty low. Because all three elastomers are amorphous polymers, their storage modulus drops sharply when the testing temperature is higher than their T_g. As might be expected, the storage modulus of all the blends are at the midlevel state. It can be recognized that the storage modulus of C25A0 is superior to C0A25, indicating that the effect of ACR on the stiffness of the blends is bigger than that of CPE.

Contact Angle Measurements

To further explore the toughening mechanism, the contact angle was measured to calculate the interfacial tension between different components of blends. There are four components in the blending system. Considering the miscibility between SAN and ASA, we herein simplify SAN and ASA as one component. The results for contact angle and surface tension are listed in Table II. The Owens–Wendt method[23] is introduced to calculate polar and dispersive tension.

The interfacial tension between different polymers can be calculated by the following equation[24]:

$$\gamma_{AB} = \gamma_A + \gamma_B - 4\gamma_A^D\gamma_B^D/\left(\gamma_A^D+\gamma_B^D\right) - 4\gamma_A^P\gamma_B^P/\left(\gamma_A^P+\gamma_B^P\right) \quad (1)$$

where γ_A and γ_B are the surface tensions of two components in contact, and γ_{AB} is the interfacial tension between component A and component B. As seen in Table III, the interfacial tensions of the CPE/(SAN/ASA), CPE/ACR, and ACR/(SAN/ASA) interfaces are 2.70, 0.74, and 4.78 mJ/m^2, respectively. Since the interfacial tension of CPE/ACR is much smaller than that of

Table II. Contact Angle and Surface Tension Results of Different Components

	Contact angle (°)		Surface tension (mJ/m^2)		
Sample	Distilled water	Diiodomethane	γ	γ^D	γ^P
SAN/ASA	77.7 ± 0.51	47.7 ± 0.59	38.60	31.42	7.18
CPE	91.9 ± 0.65	52.1 ± 0.29	33.39	31.23	2.16
ACR	99.7 ± 0.71	62.4 ± 1.02	27.23	26.06	1.19

Table III. Interfacial Energy between Different Components

Component couple	Interfacial energy (γ_{AB}) (mJ/m^2)
CPE/(SAN/ASA)	2.70
CPE/ACR	0.74
ACR/(SAN/ASA)	4.78

CPE/(SAN/ASA) and ACR/(SAN/ASA), CPE tends to interact more with ACR than with the SAN/ASA matrix, according to the thermodynamic rule that the lowest free energy is preferred. On the other hand, there is a specific interaction of hydrogen bond type between the C—Cl group in CPE and the PMMA shell of ACR.[25,26] Thus, it is conceivable that most CPE segments are surrounding the ACR in the blends.

The toughening mechanism is proposed in Figure 5. From the free-volume theories,[27] the total volume of a polymer is divided into two parts: one part is occupied by polymer molecules, called the occupied volume; the other part is the space between the molecules, called the free volume.

As shown in Figure 5, when the temperature is −30 °C, the CPE segments are "frozen out," and the free volume cannot provide enough room for the CPE segments to move. So adding CPE alone cannot have an effect on improving toughness at −30 °C. After the ACR is added individually at −30 °C, the rigid phase of the PMMA shell and SAN matrix restricts the movement of the PBA core. Thus, adding ACR alone also cannot have an obvious effect on improving toughness. However, when the ACR combines with CPE in blends at −30 °C, most CPE segments encircle the ACR. The free volume of CPE surrounding ACR provides a moving space for PBA segments that are stretching out from the PMMA shell of ACR. Hence, the toughening effect in blends containing both CPE and ACR is better than that in blends with CPE or ACR introduced individually.

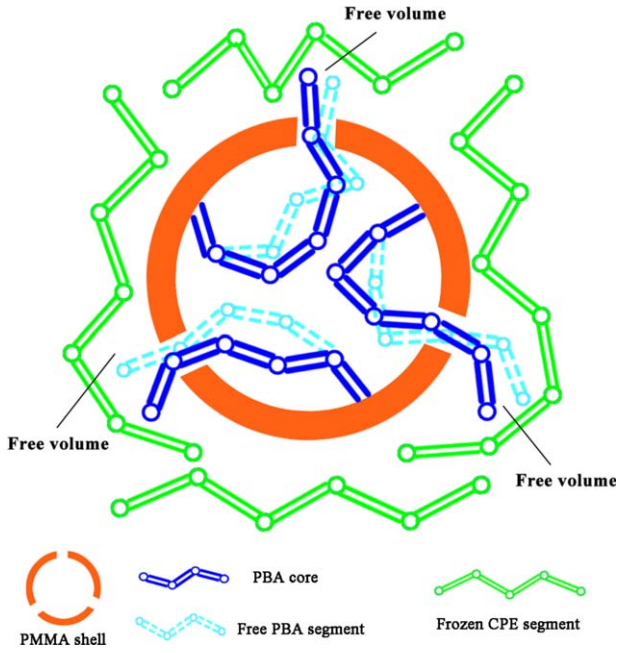

Figure 5. Schematic presentation for the toughening mechanism of CPE and ACR at −30 °C. [Color figure can be viewed in the online issue, which is available at wileyonlinelibrary.com.]

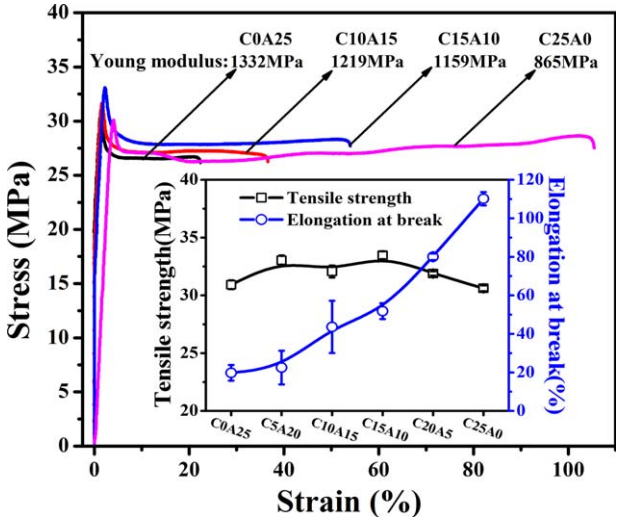

Figure 6. Tensile properties of SAN/ASA/CPE/ACR blends. [Color figure can be viewed in the online issue, which is available at wileyonlinelibrary.com.]

Furthermore, with regard to 0 and 25 °C, they are higher than the T_g of CPE. According to our previous studies,[7,11] the toughening effect of CPE was far higher than that of ACR, meaning that active movement of CPE chains was enough to significantly improve the toughness of SAN/ASA blends. Even if CPE provides moving spaces for ACR, the weak synergistic effect would be covered by the strong toughening effect of CPE at 0 and 25 °C. As a result, a synergistic effect of CPE and ACR is found at −30 °C, and not at 0 or 25 °C.

Tensile and Flexural Properties

The tensile properties of the blends acquired at 25 °C are shown in Figure 6. The tensile strength of the blends with different compositions are nearly unchanged at about 32 MPa. However, with the increasing concentration of CPE, the elongation at

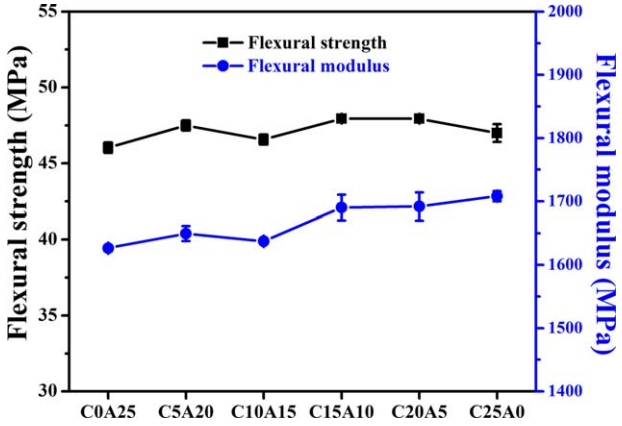

Figure 7. Flexural properties of SAN/ASA/CPE/ACR blends. [Color figure can be viewed in the online issue, which is available at wileyonlinelibrary.com.]

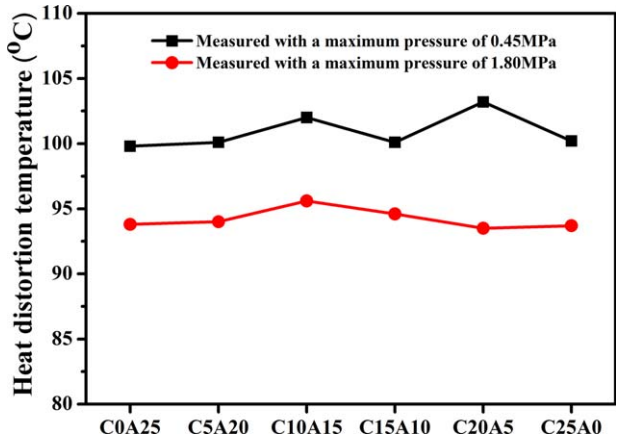

Figure 8. Heat distortion temperatures of SAN/ASA/CPE/ACR blends. [Color figure can be viewed in the online issue, which is available at wileyonlinelibrary.com.]

break grows significantly. It is well known that the elongation at break is another factor to characterize the toughness of materials.[28] In this study, elongation at break increases from 23% to 110%, indicating that the toughness of the blends is improved with the increase in CPE content at room temperature. The results for elongation at break are very consistent with the results for the impact strength. Moreover, it can be found that the Young's modulus decreases with the increasing CPE content, mainly because the rigid shells of ACR play a positive role in maintaining the values of the Young's modulus.

Figure 7 shows the flexural properties of the blends. As can be seen, with the total content of impact modifier at 25 phr, the flexural strength and flexural modulus of all blends are unchanged at about 47 MPa and 1650 MPa, respectively.

Heat Distortion Temperature

The heat distortion temperatures of the blends are shown in Figure 8. Comparing with the pure SAN/ASA (75/25) blends,[7] there is no drop in the HDTs measured at pressures of 0.45 and 1.80 MPa. The values of HDT are almost constant over all the blend compositions. Since SAN is the matrix and a continuous phase in blends and SAN is a resin with high stiffness, it plays an important role in keeping the HDT from falling. All the HDT values measured under the maximum pressure of 0.45 MPa are about 95 °C, and the HDT values measured at the maximum pressure of 1.80 MPa are all about 100 °C. Thus, the connection of two modifiers has little influence on the HDT of the blends.

CONCLUSIONS

CPE and ACR were both introduced into SAN/ASA (75/25) blends, and the total weight of CPE and ACR was kept at 25 phr. The ratio of CPE/ACR content was varied from 0/25 to 25/0. CPE played a major role in improving the impact strength of blends at 25 and 0 °C. However, an obvious synergistic toughening effect of CPE and ACR was observed at −30 °C: when the CPE and ACR were close to the same content, the impact strength of the blends reached a peak at about 7.50 kJ/m^2, which was about two to three times higher than for C25A0 and C0A25. With the increase of CPE content, the impact-fractured surfaces of the blends were more and more rough at 23 °C and 0 °C. Overlapped platelets appeared at the impact-fractured surface of C10A15 and C15A10 at −30 °C, while the impact-fractured surfaces of C0A25 and C25A0 were relatively smooth. The DMA analysis showed that the blends had three T_g values: two were in the low-temperature region, and another was in the high-temperature region. The interfacial analysis suggested that CPE segments tend to surround the ACR particles, and the free volume of CPE provided a moving space for PBA segments that were stretching out from the PMMA shell of ACR at −30 °C. Hence, the toughening effect for blends containing both CPE and ACR was better than that for blends with CPE or ACR introduced individually. Furthermore, with the total content of impact modifier maintained at 25 phr, there was little variation in the tensile strength, flexural strength, and HDT of blends.

ACKNOWLEDGMENTS

This work was supported by the Priority Academic Program Development of Jiangsu Higher Education Institutions (PAPD).

REFERENCES

1. Cai, Y.; Hu, Y.; Xiao, J.; Song, L.; Fan, W.; Deng, H.; Gong, X.; Chen, Z. *Polym.-Plast. Technol.* **2007**, *46*, 541.
2. Tolue, S.; Moghbeli, M.; Ghafelebashi, S. *Eur. Polym. J.* **2009**, *45*, 714.
3. Benson, C. M.; Burford, R. P. *J. Mater. Sci.* **1995**, *30*, 573.
4. Datta, P.; Guha, C.; Sarkhel, G. *Polym. Adv. Technol.* **2015**, *26*, 1294.
5. Edwards, S. A.; Choudhury, N. R.; Provatas, M. *J. Appl. Polym. Sci.* **2003**, *87*, 774.
6. Zhang, W.; Chen, S. J.; Zhang, J. *J. Thermoplast. Compos.* **2013**, *26*, 322.
7. Mao, Z. P.; Zhang, J. *J. Appl. Polym. Sci.* **2016**, *133*, DOI: 10.1002/app.43353.
8. Yu, J.; Feng, P.; Zhang, H. *Polym. Eng. Sci.* **2010**, *50*, 295.
9. Hassan, A.; Haworth, B. *J. Mater. Process. Tech.* **2006**, *172*, 341.
10. Guo, T.; Tang, G.; Hao, G.; Wang, S.; Song, M.; Zhang, B. *Polym. Adv. Technol.* **2003**, *14*, 232.
11. Zhang, W.; Zhang, J.; Chen, S. J. *J. Mater. Sci.* **2012**, *47*, 5041.
12. International Organization For Standardization. ISO 180, **2011**.
13. International Organization For Standardization. ISO 178, **2010**.
14. International Organization For Standardization. ISO 527, **2010**.
15. International Organization For Standardization. ISO 75, **2013**.
16. Zhou, L.; Wang, X.; Lin, Y.; Yang, J.; Wu, Q. *J. Appl. Polym. Sci.* **2003**, *90*, 916.

17. Mélo, T. J. A.; Araújo, E. M.; Brito, G. F.; Agrawal, P. *J. Alloys Compd.* **2014**, *615*, S389.
18. Hwang, I. J.; Kim, B. K. *J. Appl. Polym. Sci.* **1998**, *67*, 27.
19. Zhang, Z.; Zhao, X. J.; Zhang, J.; Chen, S. *J. Compos. Sci. Technol.* **2013**, *86*, 122.
20. Wang, R. W.; Wang, W. *J. Appl. Polym. Sci.* **2003**, *90*, 2260.
21. Zhang, W.; Zhang, J. *Polym. Sci., Ser. A* **2014**, *56*, 296.
22. Costa, L. C.; Neto, A. T.; Hage, E. *eXPRESS Polym. Lett.* **2013**, *8*, 164.
23. Xiu, H.; Bai, H.; Huang, C.; Xu, C.; Li, X.; Fu, Q. *eXPRESS Polym. Lett.* **2013**, *7*, 261.
24. Yang, H.; Zhang, X.; Qu, C.; Li, B.; Zhang, L.; Zhang, Q.; Fu, Q. *Polymer* **2007**, *48*, 860.
25. Ramesh, S.; Leen, K. H.; Kumutha, K.; Arof, A. K. *Spectrochim. Acta, Part A* **2007**, *66*, 1237.
26. Aouachria, K.; Belhaneche-Bensemra, N. *Polym. Test.* **2006**, *25*, 1101.
27. Fox, T. G.; Flory, P. J. *J. Appl. Phys.* **1950**, *21*, 581.
28. Zhang, Z.; Chen, S. J.; Zhang, J.; Li, B.; Jin, X. P. *Polym. Test.* **2010**, *29*, 995.